



15th Canadian Masonry Symposium
Ottawa, Canada
June 2-5, 2025



AI-Assisted Seismic Debris Distribution Prediction for Unreinforced Masonry Structures

Jiadaren Liuⁱ, Ersilia Giordanoⁱⁱ, and Daniele Malomoⁱⁱⁱ

ABSTRACT

Unreinforced masonry (URM) buildings are widely prevalent across North America due to their durability, cost-effectiveness, and construction simplicity. However, older and sub-standard URM structures are particularly vulnerable to seismic loads, often experiencing severe damage and catastrophic collapse. The resulting debris from such collapses poses a significant threat to the functionality of transportation systems, severely hindering critical post-disaster operations such as medical rescue and personnel evacuation. Discontinuous modeling is the most effective approach for simulating URM failure mechanisms, as it accurately captures block detachment and damage evolution. However, traditional structural analysis tools require numerous input parameters and involve high computational costs. To address these limitations, this study employs Blender, a software primarily designed for video game development, to simulate URM collapse using its integrated physics engine. While physics engines share similarities with structural analysis tools, they prioritize computational efficiency over absolute accuracy, enabling significantly faster simulations. Following an initial validation against experimental data, the Blender physics engine was used to generate a virtual experimental database, incorporating variations in key parameters such as ground motion intensity and building height. Based on the generated database, the gradient boosted decision trees (GBDT) algorithm was employed to develop debris distribution prediction models, with hyperparameter tuning performed through ten-fold cross-validation. The resulting GBDT-based model is demonstrated to reliably predict the debris distribution of URM buildings and generate debris distribution heatmaps, which can intelligently inform decision-making in post-earthquake functional recovery efforts by providing insights into potential obstruction zones, optimizing resource allocation, and enhancing the efficiency of emergency response operations.

KEYWORDS

seismic debris, unreinforced masonry, physic engines, gradient boosted decision trees

ⁱ Postdoctoral Researcher, McGill University, Montreal, Canada, jiadaren.liu@mail.mcgill.ca

ⁱⁱ Postdoctoral Researcher, McGill University, Montreal, Canada, ersilia.giordano@mail.mcgill.ca

ⁱⁱⁱ Assistant Professor, McGill University, Montreal, Canada, daniele.malomo@mcgill.ca



INTRODUCTION

Road networks play an essential role in urban social-economic development by facilitating transportation, trade, and connectivity. However, these networks are highly susceptible to disruption during seismic events due to their direct and indirect interactions with the built environment. One major vulnerability stems from collapsed buildings generating debris that blocks critical roadways [1,2], impeding traffic flow and rendering sections of the network inaccessible. This obstruction severely hampers post-earthquake emergency response, including rescue operations and resident evacuation. The restoration of road functionality in post-earthquake scenarios is thus a crucial aspect of disaster resilience and recovery planning.

Research has demonstrated that different structural types (e.g., concrete, masonry, timber, etc.) can exhibit distinct collapse mechanisms during seismic events and thus lead to varying patterns and extents of debris deposition [3]. These differences can influence the post-earthquake functionality of road networks with varying degrees of impact. Therefore, it is essential to develop debris distribution prediction models that can account for the unique characteristics of different structural types. Such models would provide critical insights for disaster management, enabling more accurate planning of rescue routes and allocation of recovery resources.

Unreinforced masonry (URM) is one of the most prevalent structural types worldwide for both residential buildings and industrial facilities. Historical earthquake events worldwide have underscored that these structures, particularly older and substandard ones, are highly vulnerable to horizontal loads, making them prone to widespread damage and collapse, resulting in extensive debris generation [4–6]. However, while significant progress has been made in predicting debris distribution for structural types like reinforced concrete [7] and confined masonry [8], this field remains limitedly explored for URM structures. Domaneschi et al. [9] studied the debris range of collapsed URM structures through an applied element method (AEM), and developed analytical models for debris range prediction through linear regression techniques. Although the simple linear function form can facilitate the comprehension and application for engineers, it cannot be guaranteed that the target function is well modeled by this preselected class. To overcome the limitations of predefined function classes, data-driven machine learning models can be employed to provide a more reliable representation of the target function, with their successful applications widely demonstrated in structural and earthquake engineering over recent decades [10–14].

In the aforementioned studies [7–9], developing debris distribution prediction tools conventionally requires extensive numerical simulations of URM collapse and debris patterns, as obtaining experimental or real-world data is often prohibitively expensive in this field. Consequently, a robust and accurate numerical model for URM collapse simulation is essential for developing analytical or simplified debris distribution prediction tools. The seismic response of URM buildings is traditionally assessed using macro-modeling approaches within the Finite Element Method (FEM) framework [15,16]. Regular geometries are often simplified using equivalent frame models [15], while complex geometries are represented as 3D continuum models [17]. However, these methods struggle to predict collapse behavior and debris distribution, as they inherently can hardly simulate large displacements or out-of-plane failures. This limitation arises because continuous models do not explicitly represent the individual masonry units and their interfaces, making it difficult to capture block separation, sliding, and rotation that govern the collapse mechanisms of URM structures. To address these limitations, a discontinuous modeling approach is required, in which masonry is represented as an assembly of blocks interacting through interface laws. Among the available techniques, the Discrete Element Method (DEM) [18] and Non-Smooth Contact Dynamics (NSCD) [19] accurately simulate collapse mechanisms but are computationally expensive, making them impractical for large-scale structures and full-collapse scenarios outside research settings [20]. The Applied Element Method (AEM),

used by Domaneschi et al. and Sediek et al. [7,9], is a hybrid approach between FEM and DEM that balances computational efficiency and accuracy. While AEM reduces computational costs compared to DEM, it still requires significantly more resources than FEM. Given the need for a large simulation database, we believe that even with AEM, running a vast number of simulations would be excessively time-consuming. For this reason, this study employs Blender, a software primarily used for video game development, which integrates a physics engine. Physics engines, commonly used in computer graphics to simulate real-world dynamics, share similarities with structural analysis software but prioritize computational efficiency over absolute accuracy, enabling significantly faster simulations. Recent research has explored the use of physics engines to simulate URM vault collapses [21] and rocking motion of URM columns [22], yet quantitative data on the collapse of entire URM structures remains scarce.

In addition, most existing studies on seismic debris distribution [3,7–9,23] focused exclusively on either the maximum debris range or a specific range that covers a fixed percentage of the total debris volume (e.g., 100% or 90%). While these approaches provide useful insights, they often fail to account for the varying threshold percentages that disrupt road transit, which can differ significantly based on case-specific requirements and local conditions. As a result, they may either underestimate or overestimate the severity of road obstructions, limiting their effectiveness in prioritizing debris removal or planning optimal emergency routes in diverse urban contexts. Thus, a more versatile approach is needed to enhance the applicability of debris distribution predictions in diverse scenarios. For example, a heatmap-based prediction method could offer a more comprehensive representation of debris distribution patterns, allowing for a rigorous evaluation of road network disruptions. Such a method would provide valuable support for assessing the resilience of urban road networks and informing post-earthquake recovery strategies.

To this end, this paper studies the seismic debris heatmap prediction for URM structures. Firstly, a physics engine-based numerical model was developed to simulate the collapse behavior and debris patterns of URM structures, which was then validated using existing experimental tests. Subsequently, the validated numerical model was utilized to generate a virtual experimental database that accounts for varying input parameters, including ground motion intensity and building height. The resulting virtual experimental database was then split into training and testing sets to facilitate the development of data-driven debris distribution prediction models, where the gradient boosted decision trees (GBDT) algorithm was employed for model development and debris heatmap generation, enabling a versatile and robust approach to debris distribution prediction.

PHYSIC ENGINE-BASED MODEL FOR URM COLLAPSE SIMULATION

The collapse behavior and debris distribution are simulated through physic engine model in Blender [24] using a simplified micro-modelling approach, where block dimensions are enlarged to include the mortar thickness. The block elements are assumed to be rigid with a prescribed mass density. In this paper, the densities for clay brick, timber lintel, and reinforced concrete (slab) are 1890 kg/m^3 , 610 kg/m^3 , and 2320 kg/m^3 , respectively. The interactions between elements are governed by a non-smooth contact law, which enforces impenetrability and incorporates a dry friction model. Parameters utilized to define this contact model and to set the analyses are summarized in Table 1. The impact between blocks is modelled as perfect plastic by setting the bounciness coefficient equal to zero, assuming that energy dissipation occurs solely due to friction. In addition, the convex hull is adopted for the collision detection shape to avoid numerical inaccuracies during the collision detection, as well as to balance accuracy and computational efficiency.

The developed physics engine model is then utilized to simulate URM collapse and validated against the experimental of a one-story URM building test by Candeias et al. [25] as shown in Figure 1. This one-story URM building had a plan dimension of $4.15 \text{ m} \times 2.50 \text{ m}$, and a maximum height of 2.75 m . It consisted of

a gabled façade and two transverse walls, constructed with hollow clay bricks (235 mm × 115 mm × 70 mm) and arranged according to the English bond pattern. Wooden lintels were placed above the windows. The main objective of Candeias et al. was to study the out-of-plane response of this structure under a unidirectional earthquake applied perpendicular to the main façade by a shaking table test. The earthquake considered in their study was adopted from the recorded ground motion that occurred near Christchurch (New Zealand) on 21 February 2011. The original ground motion of this earthquake was unable to induce structural collapse for this test and was thus scaled incrementally. When the reference signal was scaled to 300% (a PGA of 1.27g), which was achieved at the eighth increment, collapses occurred.

Table 1: Parameters in the developed physic engine model

Parameter	Unit	Adopted value
Solver iteration-steps	[step]	10
Collision Detection shape	-	Convex Hull
Collision margin	[m]	10^{-6}
Simulation sub-steps	[steps/s]	2
Simulation rate	[fps]	200
Bounciness coefficient	[%]	0.00
Friction coefficient	-	1.00 (45°)
Translational damping	-	0.00
Rotational damping	-	0.00

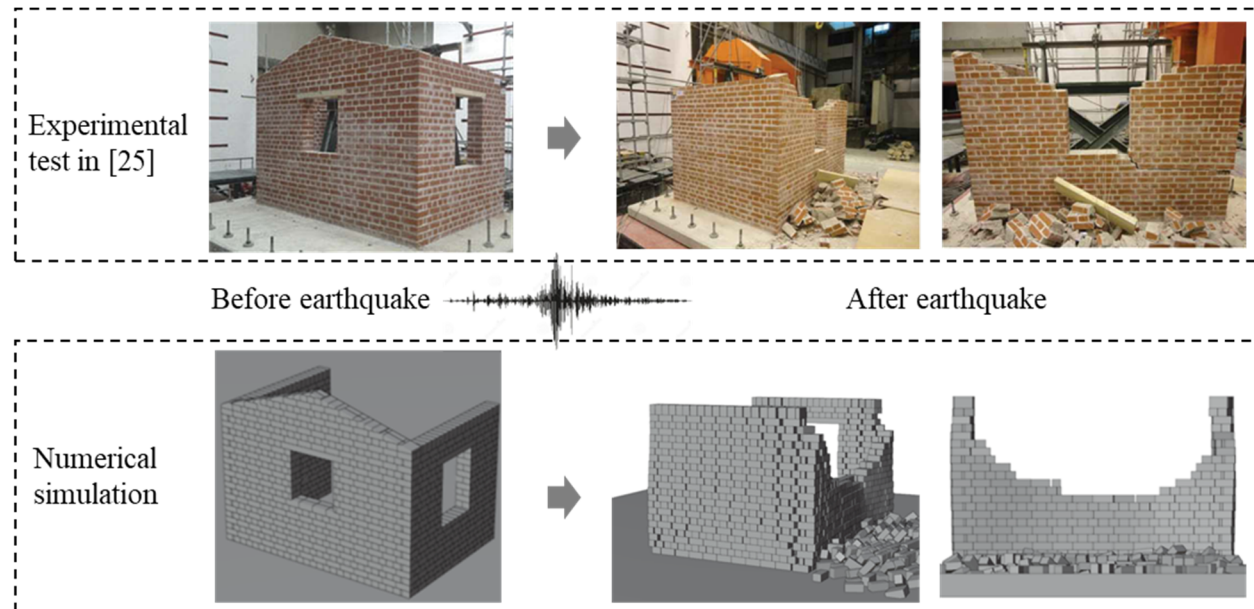


Figure 1: Comparison between experimental and numerical results

In this study, only the last experimental incremental stage is simulated, purely focusing the collapse behavior and debris distribution. It is assumed that the model being in a pre-damaged state where the mortar contribution was just lost. The same ground motion from [25] is assigned in terms of displacement time history at the base block. As shown in Figure 2, the developed model satisfactory, although not perfectly, captured the structural collapse and wall overturning behaviors. Similar damage locations and debris patterns are observed between experimental and numerical results. The results demonstrate that the

developed model can approximate the out-of-plane response of URM structures with efficient computational cost.

VIRTUAL EXPERIMENTAL DESIGN

The validated physic engine-based model is then employed to generate a virtual experimental database on seismic debris distribution. Two URM structures, the one-story building from [25], and a two storey building with the same plan dimensions as the one-story building, are modelled as shown in Figure 2. It is assumed that the two storey building is built with the same materials and technique as the one-story building from [25]. A 150 mm reinforced concrete slab floor is considered for this two-storey building, as well as a hypothesized timber-pitched roof as a common approach in URM constructions and simulations [26].

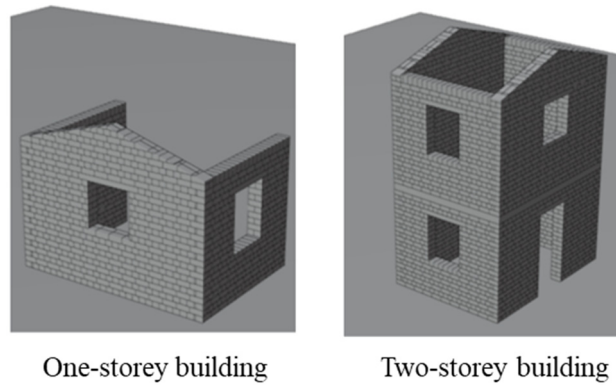


Figure 2: Building types considered in virtual experimental design

A total of 251 scenarios are simulated by considering different ground motions and building types as summarized in Table 2. The selection of ground motions is based on the intensity measure of cumulative absolute velocity (CAV), which accounts for both the amplitude and duration of ground motions and is better correlated with structural cumulative damage and collapse mechanisms compared with other intensity measures. With a wide cover range of CAV from 3.4 to 40.5, a total of 11 ground motion records are adopted from the Pacific Earthquake Engineering Research (PEER) ground motion database [27]. Similar to the experimental observations reported in [25], certain ground motion records fail to induce the full collapse of URM structures. An amplification/reduction factor of α is thus applied to each ground motion by scaling the acceleration amplitude uniformly over its entire duration, until a full collapse of URM structures is observed. For example, in Table 2, [3.75, 11, 0.25] represents numbers increasing from 3.75 to 11 with an increment of 0.25. In addition, two collapse analyses are conducted for each virtual test, applying the ground motion perpendicular and parallel to the main façade, respectively. The analysis yielding the largest debris area is then included in the virtual experimental database.

The volume and coordinates of each block are recorded throughout the URM collapse simulation process. Subsequently, the seismic debris heatmap can be generated for each simulation, as illustrated in Figure 3. The innermost rectangle represents the footprint ($a' \times b'$) of the URM building prior to collapse, while the outermost rectangle represents the expanded footprint ($a \times b$) after collapse that covers all seismic debris. This amplification factor for the footprint dimension, R , is defined as a function of critical variables in the virtual experimental design, as expressed in Eq. (1),

$$(1) R = f(CAV, h, \alpha, \beta)$$

where CAV denotes the intensity measure of ground motions, h is the number of stories, α is the scale factor applied to ground motions, and β represents the percentage of covered debris volume, ranging from 0.5 to 1.0. When $\beta = 1.0$, $R = \frac{a'}{a} = \frac{b'}{b}$, as shown in Figure 3. Using the predefined model parameters in Eq. (1), machine learning prediction models can be developed to estimate the amplification factor of R , which can subsequently be utilized to generate seismic debris heatmaps. The predicted amplification factor R is used to scale the original building footprint to define the spatial extent of debris dispersion, forming a rectangular boundary that encompasses a specified percentage of the total debris volume. This boundary is then discretized into a uniform grid to generate a debris distribution heatmap, where each cell represents the relative debris density within that area.

Table 2: Virtual experimental design matrix

Building type	Earthquake	CAV (m/s)	α
One-storey	Saguenay	3.4	40, 50, 60, 100, 200
	Hollister	4.2	[3.75, 11, 0.25]
	Southnapa	6.0	[5.75, 11, 0.25]
	Friuli	6.7	[3.25, 11, 0.25]
	Christchurch	8.3	[1.25, 4.25, 0.25]
	Morgan Hill	9.3	[2.25, 9, 0.25]
	Loma pierta	12.6	[1.75, 6.25, 0.25]
	Imperial Valley	16.4	[1.5, 6, 0.25]
	Northridge	17.9	[0.75, 3, 0.25]
	Chi-Chi	25.9	[0.75, 3, 0.25]
Nahanni	40.5	[0.25, 1, 0.25]	
Two-storey	Saguenay	3.4	50, 60, 100
	Hollister	4.2	[4.75, 8, 0.25]
	Southnapa	6.0	[8, 11, 0.25]
	Friuli	6.7	[6.25, 6.5, 0.25]
	Christchurch	8.3	[1.5, 2.5, 0.25]
	Morgan Hill	9.3	[4.25, 6, 0.25]
	Loma pierta	12.6	[2, 2.5, 0.25]
	Imperial Valley	16.4	[2.5, 3, 0.25]
	Northridge	17.9	[0.75, 2, 0.25]
	Chi-Chi	25.9	[0.5, 1.25, 0.25]
Nahanni	40.5	0.25	

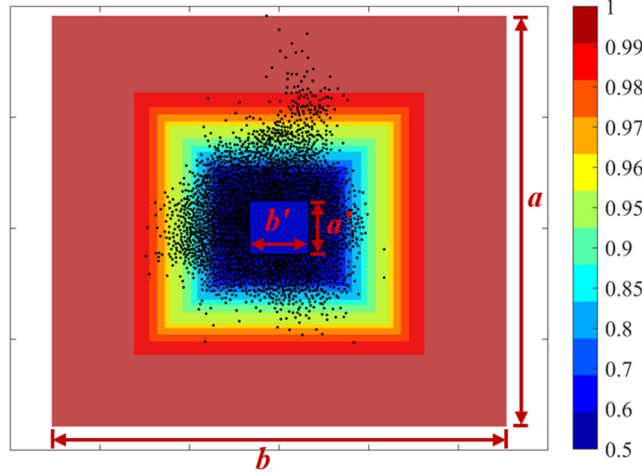


Figure 3: Seismic debris heatmap visualization

GBDT-BASED SEISMIC DEBRIS DISTRIBUTION PREDICTION

This study represents an initial stage of a broader research program, where GBDT was selected due to its strong performance in capturing nonlinear relationships and its proven robustness in small-to-medium-sized datasets. Future work will involve a systematic comparison with other machine learning algorithms commonly used in structural and earthquake engineering to identify the most effective approach for debris distribution prediction. The GBDT algorithm is an ensemble learning method that constructs models sequentially, optimizing their predictive accuracy by iteratively minimizing a predefined loss function through gradient descent. Each tree is built to correct the residual errors of its predecessor, ensuring continuous improvement in the overall model. In this study, mean squared error (MSE) was used as the loss function to guide the optimization process. Unlike random forests, where individual trees are constructed independently, GBDT trees are dependent and added sequentially, which enhances their predictive capabilities. GBDT is particularly suited for capturing complex, nonlinear relationships [28], making it a robust choice for predicting seismic debris distribution in collapsed masonry buildings.

The virtual experimental database is split into training and testing subsets with 80% and 20% of the total data, respectively. Hyperparameter tuning is then conducted for the GBDT algorithm through 10-fold cross-validations using the training dataset. The coefficient of determination, usually denoted as R^2 , is adopted as the performance evaluation metric as shown in Eq. (2),

$$(2) R^2 = 1 - \frac{\sum_{i=1}^n (y_i - \hat{y}_i)^2}{\sum_{i=1}^n (y_i - \bar{y})^2}$$

where y_i is the actual target value for the i -th observation, \hat{y}_i denotes its predicted counterpart, \bar{y} is the mean of the actual target values, and n is the total number of observations in the dataset.

Critical hyperparameters considered for tuning include learning rate ranging from 0.001 to 0.3, the number of boosting stages ranging from 50 to 500, the maximum depth of individual estimators ranging from 2 to 10, the minimum samples required to split an internal node ranging from 2 to 10, and the minimum samples required to be at a leaf node ranging from 2 to 10. Through the exhaustive grid search approach, the optimal values from these hyperparameters are 0.2, 250, 5, 2, and 2, respectively.

The performance of the developed GBDT model is evaluated on the testing dataset, as summarized in Table 3. To facilitate comparison and assess potential overfitting, the model's performance is also examined on

the training dataset. In addition to R^2 , another two widely used performance metrics, root mean squared error (RMSE) and mean absolute error (MAE), are employed, as shown in Eq. (3) and (4).

$$(3) \text{ RMSE} = \sqrt{\frac{1}{n} \sum_{i=1}^n (y_i - \hat{y}_i)^2}$$

$$(4) \text{ MAE} = \frac{1}{n} \sum_{i=1}^n |y_i - \hat{y}_i|$$

Table 3: Model performance evaluation

Training dataset			Testing dataset		
R^2	RMSE	MAE	R^2	RMSE	MAE
0.9869	0.1454	0.0851	0.9357	0.3035	0.1543

The developed GBDT model demonstrates strong performance on the testing dataset, achieving an R^2 value of 0.9357, where an R^2 value of 1.0 indicates perfect accuracy. As expected, the model performs slightly better on the training dataset, but no significant overfitting is observed. The evaluation metrics, R^2 , RMSE, and MAE, show consistent results, with lower RMSE and MAE scores corresponding to higher R^2 values. These findings indicate that the developed GBDT model is a reliable tool for predicting seismic debris distribution in URM structures and generating seismic debris heatmaps, which can aid in prioritizing debris removal strategies, enhancing the efficiency of post-earthquake road network recovery, and supporting comprehensive resilience assessments of affected regions.

CONCLUSIONS

This study presented a preliminary framework for accurately predicting the debris distribution of URM buildings to mitigate their impact on transportation systems and facilitate efficient post-disaster operations. A physics engine-based numerical model was developed and validated using existing experimental data to simulate collapse behavior and debris patterns, based on which a virtual experimental database on URM collapse and debris distribution was generated.

Leveraging this database, the GBDT algorithm was employed to predict seismic debris distribution and generate distribution heatmaps. The developed model achieved strong predictive performance, with an R^2 value of 0.9357 on the testing dataset, demonstrating its accuracy and generalization capability. Evaluation results from multiple metrics, including RMSE and MAE, were consistent, and no significant overfitting issues were observed.

The developed models can be utilized to inform post-earthquake functionality recovery of road networks and resilience assessment of affected regions. By optimizing resource allocation and enhancing the efficiency of emergency response operations, the developed GBDT model provides a critical tool for improving disaster preparedness and accelerating recovery efforts in urban environments vulnerable to seismic hazards. In the next stage of this research program, more machine learning algorithms will be employed to evaluate their performance and compared with the GBDT algorithm in this manuscript, where more comprehensive insights on debris distribution prediction are expected to be revealed.

ACKNOWLEDGEMENTS

The authors acknowledge the support of the Natural Sciences and Engineering Research Council of Canada (NSERC) [funding reference number RGPIN-2022-03635].

REFERENCES

- [1] Shang Q, Guo X, Li J, Wang T. Post-earthquake health care service accessibility assessment framework and its application in a medium-sized city. *Reliab Eng & Syst Saf* 2022;228:108782.
- [2] Wu Y, Chen S. Traffic resilience modeling for post-earthquake emergency medical response and planning considering disrupted infrastructure and dislocated residents. *Int J Disaster Risk Reduct* 2023;93:103754.
- [3] He Y, Zhai C, Wen W. Probabilistic prediction of post-earthquake rubble range for RC frame structures. *Soil Dyn Earthq Eng* 2023;171:107927.
- [4] Eschenasy D. Collapses of masonry structures under non-extreme loads. *Improv. Seism. Perform. Exist. Build. Other Struct.* 2015, 2015, p. 353–62.
- [5] Sun B, Yan P. Damage characteristics and seismic capacity of buildings during Nepal M s 8.1 earthquake. *Earthq Eng Eng Vib* 2015;14:571–8.
- [6] Liu J, Scattarreggia N, Malomo D. Exploring the seismic performance of corroded RC frames with masonry infills. *Bull Earthq Eng* 2024:1–26.
- [7] Sediek OA, El-Tawil S, McCormick J. Seismic debris field for collapsed RC moment resisting frame buildings. *J Struct Eng* 2021;147:4021045.
- [8] He Y, Zhai C, Wen W, Zhang C. Probabilistic prediction of post-earthquake rubble distribution range for masonry structures. *J Build Eng* 2024;95:110208.
- [9] Domaneschi M, Cimellaro GP, Scutiero G. A simplified method to assess generation of seismic debris for masonry structures. *Eng Struct* 2019;186:306–20.
- [10] Huang C, Li Y, Gu Q, Liu J. Machine learning--based hysteretic lateral force-displacement models of reinforced concrete columns. *J Struct Eng* 2022;148:4021291.
- [11] Liu J, Alexander J, Gu Q, Li Y. Gaussian process regression-based load-carrying capacity models of corroded prestressed concrete bridge girders for fast-screening and reliability-based evaluation. *Eng Struct* 2023;285:116040.
- [12] Li S, Li C, Huang Y, Zhai C. Real-time seismic damage simulation for urban building portfolio based on basic building information and machine learning. *Int J Disaster Risk Reduct* 2024;111:104687.
- [13] Liu J, Alexander J, Li Y. Gaussian Process Regression--Based Model Error Diagnosis and Quantification Using Experimental Data of Prestressed Concrete Beams in Shear. *ASCE-ASME J Risk Uncertain Eng Syst Part A Civ Eng* 2025;11:4024095.
- [14] Liu J, Alexander J, Li Y. Probabilistic error assessment and correction of design code-based shear strength prediction models for reliability analysis of prestressed concrete girders. *Eng Struct* 2023;279:115664.
- [15] Lagomarsino S, Penna A, Galasco A, Cattari S. TREMURI program: An equivalent frame model for the nonlinear seismic analysis of masonry buildings. *Eng Struct* 2013;56:1787–99. <https://doi.org/10.1016/j.engstruct.2013.08.002>.
- [16] D'Altri AM, Sarhosis V, Milani G, Rots J, Cattari S, Lagomarsino S, et al. A review of numerical models for masonry structures. *Numer. Model. Mason. Hist. Struct.*, Elsevier; 2019, p. 3–53. <https://doi.org/10.1016/B978-0-08-102439-3.00001-4>.
- [17] Giordano E, Clementi F, Nespeca A, Lenci S. Damage Assessment by Numerical Modeling of Sant'Agostino's Sanctuary in Offida During the Central Italy 2016–2017 Seismic Sequence. *Front Built Environ* 2019;4. <https://doi.org/10.3389/fbuil.2018.00087>.
- [18] Lemos J V. Discrete Element Modeling of Masonry Structures. *Int J Archit Herit* 2007;1:190–213. <https://doi.org/10.1080/15583050601176868>.
- [19] Chetouane B, Dubois F, Vinches M, Bohatier C. NSCD discrete element method for modelling masonry structures. *Int J Numer Methods Eng* 2005;64:65–94. <https://doi.org/10.1002/nme.1358>.
- [20] Davis L, Malomo D. Pragmatic meso-scale seismic collapse analysis of old Dutch masonry church. *Earthq Eng Struct Dyn* 2023.
- [21] Beatini V, Royer-Carfagni G, Tasora A. A regularized non-smooth contact dynamics approach for

- architectural masonry structures. *Comput Struct* 2017;187:88–100. <https://doi.org/10.1016/j.compstruc.2017.02.002>.
- [22] Ma QT, Parshottam S, Montalla M. Modelling rocking behaviour using physics engine simulation. vol. 2. 2018.
- [23] Argyroudis S, Selva J, Gehl P, Pitilakis K. Systemic seismic risk assessment of road networks considering interactions with the built environment. *Comput Civ Infrastruct Eng* 2015;30:524–40.
- [24] Mullen T. *Bounce, tumble, and splash!: simulating the physical world with Blender 3D*. John Wiley & Sons; 2008.
- [25] Candeias PX, Campos Costa A, Mendes N, Costa AA, Lourenço PB. Experimental Assessment of the Out-of-Plane Performance of Masonry Buildings Through Shaking Table Tests. *Int J Archit Herit* 2017;11:31–58. <https://doi.org/10.1080/15583058.2016.1238975>.
- [26] Malomo D, Pinho R, Penna A. Simulating the shake table response of unreinforced masonry cavity wall structures tested to collapse or near-collapse conditions. *Earthq Spectra* 2020;36:554–78. <https://doi.org/10.1177/8755293019891715>.
- [27] Goulet CA, Kishida T, Ancheta TD, Cramer CH, Darragh RB, Silva WJ, et al. PEER NGA-east database. *Earthq Spectra* 2021;37:1331–53.
- [28] Di B, Zhang H, Liu Y, Li J, Chen N, Stamatopoulos CA, et al. Assessing susceptibility of debris flow in southwest China using gradient boosting machine. *Sci Rep* 2019;9:12532.